Modeling barrier properties of intestinal mucus reinforced with IgG and secretory IgA against motile bacteria

Feifei Xu[1], Jay M. Newby[1], Jennifer L. Schiller[2], Holly A. Schroeder[2], Timothy Wessler[1], Alex Chen[1], M. Gregory Forest[1,3*], Samuel K. Lai[2-4*]

[1] Departments of Mathematics and Applied Physical Sciences, University of North Carolina – Chapel Hill, 120 E Cameron Ave, Chapel Hill, NC 27599-3250
[2] Division of Pharmacoengineering and Molecular Pharmaceutics, Eshelman School of Pharmacy, University of North Carolina – Chapel Hill, 125 Mason Farm Rd, Chapel Hill, NC 27599
[3] UNC/NCSU Joint Department of Biomedical Engineering, University of North Carolina – Chapel Hill, Chapel Hill, NC 27599
[4] Department of Microbiology & Immunology, University of North Carolina – Chapel Hill, Chapel Hill, NC 27599, USA
* Corresponding authors: lai@unc.edu, forest@unc.edu

Keywords: mucin, immunoglobulins, mucosal immunity, pathogen

The gastrointestinal (GI) tract is lined with a layer of viscoelastic mucus gel, characterized by a dense network of entangled and crosslinked mucins together with an abundance of antibodies (Ab). Secretory IgA (sIgA), the predominant Ab isotype in the GI tract, is a dimeric molecule with 4 antigen-binding domains capable of inducing efficient clumping of bacteria, or agglutination. IgG, another common Ab at mucosal surfaces, can crosslink individual viruses to the mucin mesh through multiple weak bonds between IgG-Fc and mucins, a process termed muco-trapping. The relative contributions by agglutination vs. muco-trapping in blocking permeation of motile bacteria through mucus remains poorly understood. Here, we developed a mathematical model that takes into account physiologically relevant spatial dimensions and time scales, binding and unbinding rates between Ab and bacteria as well as between Ab and mucins, the diffusivities of Ab, and run-tumble motion of active bacteria. Our model predicts both sIgA and IgG can accumulate on the surface of individual bacteria at sufficient quantities and rates to enable trapping individual bacteria in mucins before they penetrate the mucus layer. Furthermore, our model predicts that agglutination only modestly improves the ability for antibodies to block bacteria permeation through mucus. These results suggest that while sIgA is the most potent Ab isotype overall at stopping bacterial penetration, IgG may represent a practical alternative for mucosal prophylaxis and therapy. Our work improves the mechanistic understanding of Ab-enhanced barrier properties of mucus, and highlights the ability for muco-trapping Ab to protect against motile pathogens at mucosal surfaces.

All exposed surfaces in the human body not covered by skin, including those of the respiratory, gastrointestinal (GI), and urogenital tracts, are covered with mucus that is continuously cleared and replenished.[1] In addition to the dense network of mucins, mucus also contains various proteins, lipids, shed cells, and ions, all of which contribute to its viscoelastic rheological profile and microstructural properties essential for a multitude of biological functions.[1] Along the GI tract, mucus not only functions as a lubricant that facilitates the transport of chyme, but also as a continuously renewed physical barrier capable of preventing foreign particulates and pathogens from harming the underlying epithelium.[1]

The physical barrier properties of native mucus against foreign pathogens are rooted in steric obstruction by the dense mucin mesh, as well as adhesive interactions with mucins. In addition, this "baseline" physical barrier can be further reinforced with antigen-specific antibodies (Ab) secreted by the immune system, including IgG and secretory IgA (sIgA).[2-6] Indeed, more Ab are secreted into mucus than into blood and lymph,[7] underscoring a likely role for secreted Ab to reinforce the mucus barrier against foreign pathogens, and consequently facilitate protection. It has long been shown that multimeric Ab such as sIgA and IgM can agglutinate pathogens into large aggregates that are too large to permeate through mucus, a phenomenon also referred to as immune exclusion.[8-9] sIgA was also found to interact with mucins.[10-11] It was not until recently that viral antigen-specific IgG was shown to potently immobilize individual viruses in mucus through multiple weak and transient bonds between the array of virion-bound IgG and mucins,[12-15] akin to a Velcro® patch; this process is referred to as muco-trapping. Regardless of whether pathogens are agglutinated or individually trapped in mucus, reduced pathogen mobility across mucus directly reduces the flux of pathogens reaching target cells in the epithelium[12-13] and thereby facilitates rapid elimination by natural mucus clearance mechanisms.[12, 15]

The GI mucosa is continuously exposed to a diverse spectrum of commensal and pathogenic bacteria. Although most bacteria do not require human host cells to replicate, bacteria generally must be in close proximity to cells to exert toxicity.[16] Similar to viruses that undergo rapid diffusion in mucus, there is only a limited window of opportunity during which Ab must accumulate on a bacterium at sufficient quantities to immobilize the bacterium before it can swim through mucus.[12] Unlike the Brownian motion of viruses, many bacteria utilize active flagella to propel themselves, leading to markedly faster passage times through mucus than viruses.[17-18] At the same time, the larger size of bacteria and the greater number of surface epitopes inevitably lead to greater rates and numbers of Ab bound per bacterium. Understanding this subtle interplay between the various kinetic, diffusive, and advective processes, as well as comparing the relative contributions of muco-trapping vs. agglutination in limiting bacterial penetration through physiologically thick mucus layers, are exceedingly challenging

to study experimentally. Instead, here we turned to computational modeling to elucidate the effectiveness of Ab-reinforced barrier properties of mucus against highly motile bacterial pathogens (Figure 1). Details of this model can be found in the Experimental section.

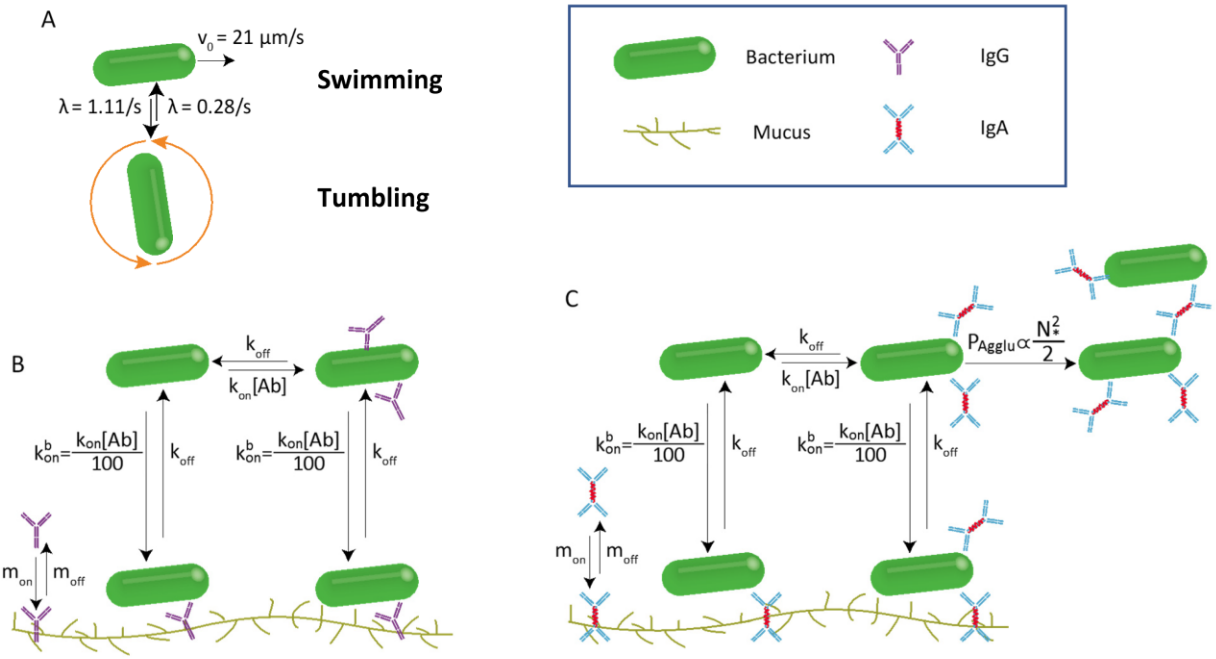

Figure 1. Schematic of our model. **(A)** Motile bacterium switches between run and tumbling states. **(B)** IgG interact with mucus, bind bacteria, and facilitate muco-trapping of bacteria. **(C)** In addition to muco-trapping, sIgA can induce bacterial agglutination.

Results

Modeling bacterial penetration of mucus layers without Ab

We sought to first determine the rates with which active bacteria can penetrate physiologically thick mucus layers in the absence of bacteria-binding Ab. To ensure physiological relevance, we input model parameters that reflect the run-and-tumble motion of *Salmonella typhimurium* in fresh mouse GI mucus measured *ex vivo* (Supplemental Video 1), which on average exhibited a run phase of ~0.9s with an effective velocity of 21 µm/s and a tumble phase of ~3.6s. The thickness of the mucus layer varies substantially throughout the GI tract, ranging from as little as ~50 µm in the duodenum to over 800 µm in the colon.[19] Not surprisingly, for a relatively thin mucus layer, e.g. 150 µm, the vast majority of bacteria (>90%) can swim through the mucus and reach the underlying epithelium within 15 mins (Figure 2A). As the mucus layer thickness increases, fewer bacteria permeate through the mucus layer, with less than 20% of the bacteria capable of penetrating across a 450 µm thick mucus layer within the same time period (Figure 2B-C). Over longer durations (e.g. 60 mins), the majority of bacteria are still

able to penetrate through GI mucus (Figure 2C). Since mucus clearance in the GI tract typically occurs on the order of hours, these results suggest that native GI secretions alone, in the absence of innate antimicrobial molecules that can directly inactivate the bacteria, are unlikely to pose an effective barrier blocking the permeation of active bacteria.

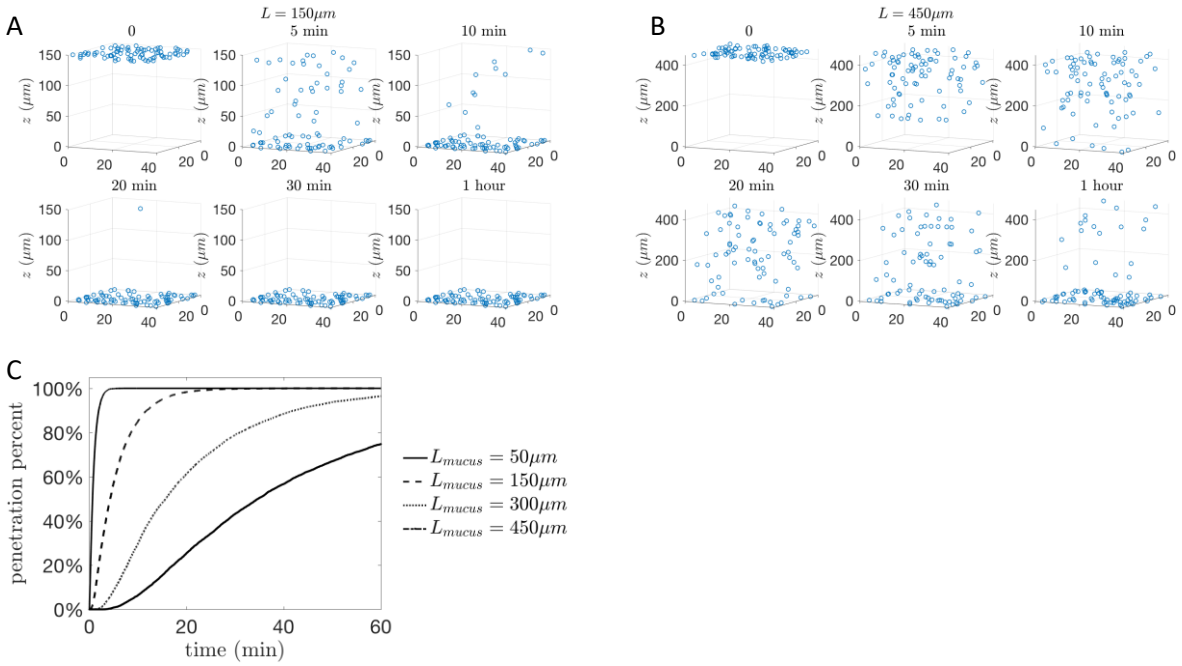

Figure 2. Simulations of bacterial penetration of mucus layers in the absence of bacteria-binding Ab. **(A-B)** Representative distribution of the position of bacteria after 0 min, 5 min, 10 min, 20 min, 30 min and 1 hr assuming **(A)** $L_{mucus} = 150\ \mu m$ and **(B)** $L_{mucus} = 450\ \mu m$. All bacteria are initially randomly placed in the most luminal 5 µm layer, "run" with a velocity of $v = 21\ \mu m/s$ for duration $\mu_{run} = 0.9s$, and "tumble" for duration $\mu_{tumble} = 3.6s$. **(C)** Total fraction of bacteria that can reach the underlying epithelium over time for several mucus layer thicknesses.

Modeling bacterial penetration of mucus layers containing antigen-specific IgG

Despite exceptionally weak affinity to mucins (IgG was previously shown to be slowed ~10-20% in mucus gel compared to in buffer)[13, 20-21] virus antigen-specific IgG was able to effectively immobilize viruses undergoing Brownian diffusion in mucus.[13] This motivated us to model whether the presence of bacterial antigen-specific IgG may immobilize individual bacteria in mucus and substantially reduce their penetration rates across the mucus layer. Since both IgG and virus undergo Brownian motion, the extent to which additional IgG bound to virus can reduce virus mobility in mucus can be easily modeled.[22] Unfortunately, the extent to which a single bacterium-bound IgG may slow bacterial velocity when it transiently associates with mucins is not known. We thus made the conservative first-order estimate that each IgG would slow bacterial velocity by 1%, or 10-fold less effective than slowing viruses. Even with such weak IgG-mucin affinity, and assuming relatively sparse antigen density on the bacteria, our

model suggests that modest concentrations of IgG (10-20 µg/mL) could effectively immobilize individual bacteria in the mucus gel and in turn substantially reduce the bacterial flux through mucus (Figure 3A-B, vs. Figure 2A). Our observations are in good agreement with experimental observations showing immobilizing of individual *Salmonella* bacteria in mouse GI mucus (Supplemental Video 2). Since individual IgG molecules only possess weak affinity to mucins, IgG-mediated trapping of motile bacteria is a direct consequence of the rapid accumulation of IgG on the bacteria: within minutes, dozens if not hundreds of IgG are bound to the surface of each bacteria, which collectively exert high avidity adhesive interactions with the mucin mesh (Figure 3C). With 10 µg/mL of antigen-specific IgG in mucus, the model estimates the fraction of bacteria that can swim through mucus is reduced to 26%, 1%, and 0.025% when the mucus layer is 150 µm, 300 µm, and 450 µm thick, respectively (Figure 3D), reflecting a decrease of ~78%, ~95%, and ~75% compared to no Ab control (Figure 3E).

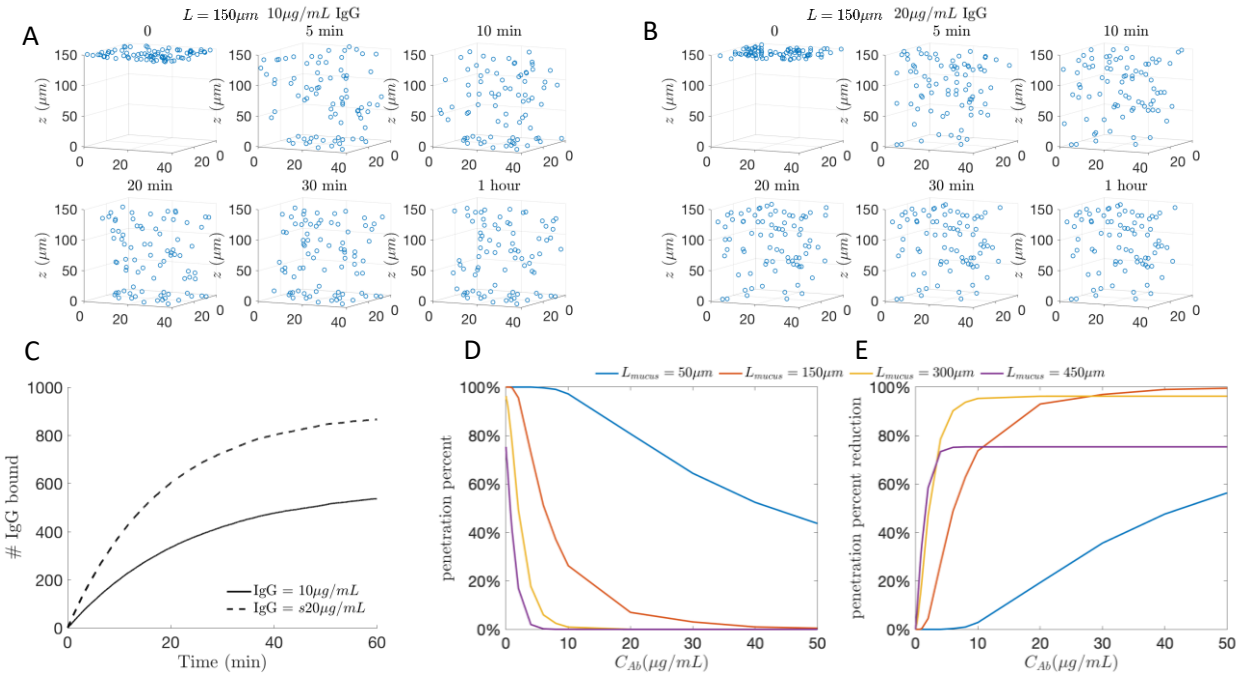

Figure 3. Simulations of bacterial penetration of mucus layer containing bacteria-specific IgG. **(A - B)** Representative distribution of spatial locations of simulated bacteria after 0 min, 5 min, 10 min, 20 min, 30 min, and 1 hr in a 150 µm thick mucus layer containing **(A)** 10 µg/mL and **(B)** 20 µg/mL IgG. All bacteria are initially randomly placed in the most luminal 5 µm layer, "run" with a velocity of $v = 21\ \mu m/s$ for $\mu_{run} = 0.9s$, and "tumble" for $\mu_{tumble} = 3.6s$. **(C)** The average number of IgG bound to bacteria over time. **(D)** Fraction of bacteria that can penetrate across mucus layers of different thickness across different IgG concentrations within one hour post bacterial inoculation. **(E)** The extent of reduction in bacterial penetration across different IgG concentrations compared to no IgG control for different mucus layer thickness.

Intuitively, greater concentrations of IgG in mucus would lead to greater trapping potency. In our simulation, this is dependent on both the IgG concentration and the thickness of the mucus layer.

When the mucus layer is relatively thin (e.g. 150 μm), increasing the IgG concentration proportionally reduces the bacterial flux through mucus. As the thickness of the mucus layer increases, further increases in the IgG concentration beyond ~10-20 μg/mL did not appreciably reduce the bacterial flux (Figure 3D-E). First, it takes an identically active bacterium longer time to penetrate through thicker mucus layers, making it more likely a critical threshold of bacterium-bound IgG is reached for the bacterium to become immobilized in mucus before it successfully swims across the mucus gel. Thus, as the thickness of the layer is increased, the IgG concentration needed to achieve the same reduction in the fraction of bacteria reaching the underlying epithelium is decreased (Figure 3E; Supplemental Figure 1). These results underscore the potential effectiveness with which physiological concentrations of IgG can reinforce physiologically thick mucus layers against highly motile bacterial species.

Modeling bacterial penetration of mucus layers containing antigen-specific sIgA

The predominant Ab isotype in the GI mucosa is sIgA. In addition to monomeric IgA exhibiting similar affinity to mucins as IgG,[20-21] the secretory component (SC) of sIgA is also thought to possess affinity to mucins.[23] Furthermore, the dimeric nature of sIgA, with 4 Fab arms in opposite directions vs. 2 Fab arms on IgG, makes sIgA much more potent at crosslinking multiple bacteria than IgG.[2, 24] Bacteria that are bound to each other cannot effectively employ propulsion by flagella; this phenomenon, commonly referred to as agglutination, is fundamentally different than trapping of individual bacteria due to multiple low-affinity bonds between mucins and bacteria-bound Ab. We thus modeled the extent to which sIgA, which can facilitate both efficient agglutination and muco-trapping, can enhance the mucus barrier over IgG.

Agglutination depends not only on the concentration of multimeric Ab such as sIgA and IgM, but also on the concentrations and mobility of the pathogen. For instance, numerical simulations and theoretical analysis indicate that the concentrations of HIV in semen – even those from acutely infected individuals possessing the highest viral titers – were insufficient for appreciable fractions of HIV to encounter another HIV virion before the majority of the virions can diffuse across the mucus layer.[25] By definition, HIV cannot be efficiently agglutinated. This finding corroborated experimental studies that failed to observe appreciable agglutination of viruses or virus-sized nanoparticles in mucus, even with the pentameric IgM.[26] Nevertheless, bacteria not only are present at greater concentrations than viruses, but also possess substantially greater mobility (due to swimming/run phases that dominate over diffusive/tumbling phases) than viruses. Hence, active bacteria are much more likely to experience encounters with each other than viruses.

To begin to estimate the impact of agglutination, we first simulated the encounter (or collision) frequency originating from run/tumble motions of active bacteria, defined as the frequency with which two bacteria are separated by a distance less than the dimension of a single sIgA molecule. We placed bacteria randomly in the most luminal 5 µm of the mucus layer, and counted the collisions of tracked bacteria with other bacteria. Naturally, the average distance of a bacterium to its closest neighbor is shortest at time t=0; as time passes and bacteria begin to spread, the average distance to its closest neighbor begins to increase (Supplemental Figure 2A-F), which in turn directly reduces the collision frequency over time (Supplemental Figure 2G).

The rate of bacterial agglutination is a direct product of the frequency of collisions between two sIgA-bound bacteria, and the number of collisions before sIgA bound on one bacterium successfully binds to an unbound antigen on the second bacteria. Although it has been previously shown that roughly one in one hundred collisions between an antibody and an antigen target results in a successful bond, the precise kinetics of sIgA-mediated agglutination remains poorly understood. To arrive at a first order estimate of the potency of agglutination, we assumed the extreme scenario whereby each collision between two bacteria with optimal density of surface bound sIgA results in a successful crosslink. At this theoretical limit of extreme crosslinking efficiency, sIgA-induced agglutination further reduces the bacterial flux compared to equal amounts of IgG across all sIgA concentrations and mucus layer thickness (Figure 4). In the presence of 10 µg/mL IgG, the average distance the bacteria penetrate into the mucus before becoming immobilized is ~85 µm, whereas that distance is reduced to ~75 µm in the presence of 10 µg/mL sIgA. A similar trend is seen with greater Ab concentration; the average distance the bacteria penetrates into the mucus layer before becoming immobilized is ~60 µm with 20 µg/mL IgG vs. ~48 µm for 20 µg/mL sIgA. Notably, the Ab isotype or concentration does not affect the rate of penetration within the first minute, but the subsequent maximal depth of bacterial penetration is reached within ~2 mins with 20 µg/mL sIgA. Conversely, 10 µg/mL IgG reach equilibrium 10 minutes later. Without antibody, the bacteria completely penetrate mucus 150 µm thick in under 20 minutes.

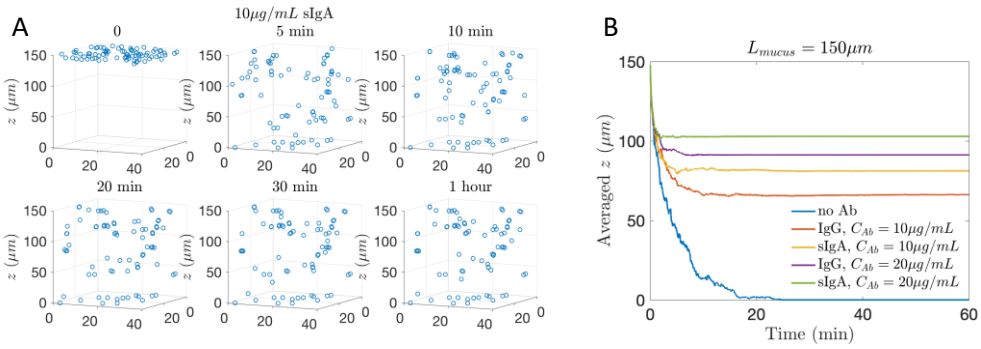

Figure 4. Simulations of bacteria penetration of mucus layer containing bacteria-specific sIgA. **(A)** Representative distribution of spatial locations of simulated bacteria after 0 min, 5 min, 10 min, 20 min, 30 min, and 1 hr in a 150 µm thick mucus layer containing 10 µg/mL of sIgA with 100% agglutination efficiency. **(B)** The average distance from the bottom of the mucus layer for all bacteria in the simulation versus time.

The improvement afforded by agglutination is increasingly diminished with increasing mucus thickness. When we decrease the agglutination efficiencies from this theoretical extreme, the additional benefit of agglutination afforded by sIgA vs. trapping of individual bacteria (i.e. IgG) begins to disappear. With an agglutination efficiency such that two bacteria would need to undergo on average 10 collisions with each other before becoming bound together, there is negligible difference between sIgA and IgG in reducing the flux of bacteria penetrating across the mucus layer across a variety of mucus thickness and Ab concentrations (Figure 5). The concentration of Ab required to impede bacterial penetration instead depends to a greater extent on mucus layer thickness; in mucus of thickness 150 µm, 300 µm, and 450 µm, bacterial penetrance is completely prevented at Ab concentrations of 45 µg/mL, 10µg/mL, and 5 µg/mL, respectively.

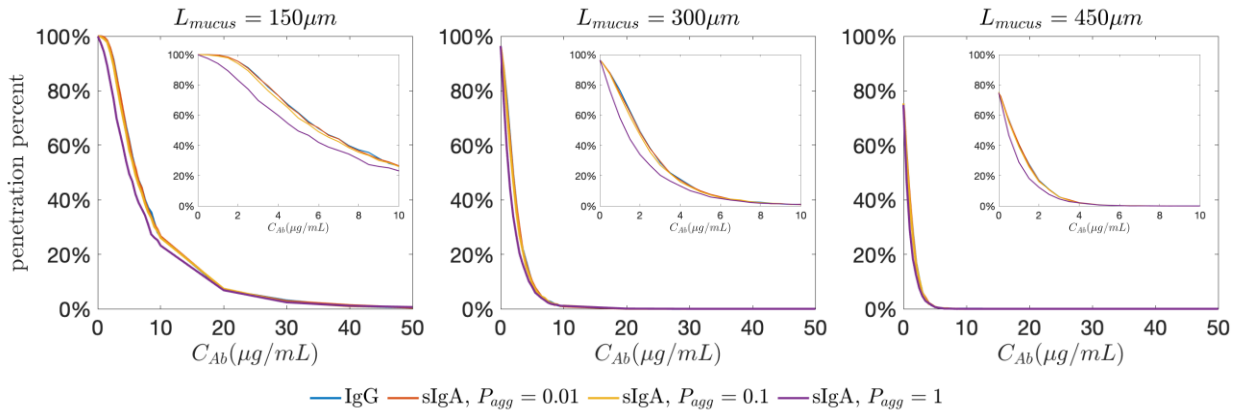

Figure 5. The fraction of bacteria that can penetrate across mucus layers containing different amounts of IgG or sIgA when the thickness of the layer is **(A)** 150 µm, **(B)** 300 µm, and **(C)** 450 µm. For sIgA, the kinetics of agglutination varies between one successful crosslink when two bacteria collide only once (P_{agg} = 1), one successful crosslink when two bacteria collide on average ten times (P_{agg} = 0.1) or on average one hundred times (P_{agg} = 0.01).

Discussion

Mucus serves as the first line of defense separating the epithelium from invasive foreign pathogens and particulates. In general, viruses and bacteria must penetrate through the mucus layer to infect or exert toxicity; it is not surprising that most pathogens have evolved a variety of mechanisms to enable their rapid permeation through mucus, including surfaces that evade adhesive interactions with mucins and an active motility apparatus such as beating flagella.[16, 18] Despite their active motility, many investigators have reported that bacteria are generally concentrated in the most luminal fraction of the mucus layer, and that the inner mucus layer is largely devoid of bacteria [3, 27-28]. This observation implies alternative mechanisms must exist to enable mucus to serve as an effective physical barrier against

highly motile bacteria. To date, the suggested mechanisms include a greater density of mucins in the inner adherent mucus layer[29] and host- or bacterial- derived defense mechanisms such as antimicrobial peptides that directly inactivate bacteria. Here, despite very conservative assumptions on antigen density, Ab-mucin affinity, and Ab-antigen affinities, we demonstrated the theoretical potency with which IgG and sIgA can immobilize motile bacteria in mucus, thereby blocking bacteria from entering the inner mucus layers and restricting them to only the most luminal mucus layers. These results underscore using topically dosed or vaccine-elicited Ab as a potentially effective yet rarely harnessed strategy to reinforce the mucus gel- our bodies' first line of defense against foreign pathogens in the GI tract.

Some investigators postulated that mucins in the mucus gel can directly bind and adhesively capture pathogens. In our opinion, it is exceedingly unlikely that direct adhesive interactions with mucins that are biochemically well conserved can effectively block the transport of the full diversity of pathogens encountered in nature, particularly because pathogens can quickly evolve. Indeed, we and others have observed both viral and bacterial pathogens can readily penetrate mucus secretions.[13-15, 17-18, 30-34] A more likely strategy to reinforcing the adhesive barrier properties of mucus is to utilize "third party" Ab molecules that can crosslink pathogens to the matrix network formed by entangled and crosslinked mucin fibers. Ab appeared well suited for this role, since our immune system can quickly develop high affinity Ab against diverse pathogens through somatic hypermutation and affinity maturation, suggesting pathogen-specific Ab could ensure that adhesive barrier properties of mucus can continually adapt to the molecular characteristics of invasive pathogens. Although bacteria can readily swim through mucus, their substantial size offers abundant antigen targets for Ab to quickly accumulate on the surface of the bacteria, leading to sufficient Ab-mucin crosslinks that result in immobilization of individual bacteria in the most luminal mucus layer.

Relative to trapping individual bacteria, the additional impact of agglutination on the overall reduction in flux of bacteria arriving at the epithelium appears modest at best under the scenario we modeled. Indeed, the additional impact of agglutination further decreases with increasing mucus layer thickness and with increasing sIgA concentrations, likely because of two factors. First, with either greater sIgA concentrations or additional time necessary to penetrate through thicker mucus layers, the result is that more sIgA will accumulate on bacteria to slow and eventually immobilize them individually. The consequent slowdown of bacteria reduces their probability to encounter another bacterium and become agglutinated. Second, bacteria that could most quickly penetrate thicker mucus layers would also be markedly less likely to encounter another bacterium once it penetrates an appreciable distance into the mucus layer, and thus agglutination would not be an effective mechanism of stopping this

subpopulation of bacteria. In general, once sIgA concentrations exceeds ~10-20 μg/mL, the reduction in bacterial flux by both agglutination and trapping (i.e. sIgA) appears indistinguishable compared to trapping individual bacteria (i.e. IgG) alone. Our model predictions are consistent with the empirical observation that IgA-deficient individuals generally do not report greater incidence of GI complications or greater susceptibility to bacterial infections than healthy individuals.[35]

Numerous studies have shown sIgA to be vital for maintaining bacterial homeostasis in the GI tract,[2, 25, 36] suggesting that sIgA likely confers other advantages beyond directly reinforcing the mucus barrier. Specific IgA-bacteria interaction combined with nonspecific IgA-mucosal interaction has been found to allow for long-term residence of commensal bacteria in the gastrointestinal tract of mice.[36] At concentrations of bacteria too low to allow for agglutination, sIgA can enchain dividing bacteria to prevent separation, impeding further division.[37] The oligosaccharides of the secretory component of non-specific sIgA have been found to competitively inhibit pathogen binding to host cells.[25] Finally, sIgA plays an important role in the regulation of immune response in the gut. Antigen-sIgA complexes can be selectively retro-transported across M cells into intestinal Peyer's patches via Dectin-1 receptors, followed by interactions with dendritic cells to induce an immunomodulatory response[2] that is anti-inflammatory due to the suppression of pro-inflammatory cytokines.[25] Should bacteria penetrate the epithelial lining and be opsonized by dimeric IgA in the lamina propia, co-activation of dendritic cells positive for Fcα receptor I with dIgA and sIgA immune complexes can also induce an inflammatory response.[38]

The amounts and relative abundance of different Ab type (i.e. IgG, sIgA, IgM) vary depending on the mucosal organ, ranging from IgG as the dominant immunoglobulin in cervicovaginal mucus to sIgA as the dominant immunoglobulin in GI mucus.[4-6] However, the conventional paradigm continues to associate immune protection at all mucosal surfaces with sIgA. The challenge with developing applications using sIgA is its notoriously poor stability and the difficulty in manufacturing and purifying in large quantities. In contrast, IgG is the easiest Ab class to manufacture and store.[39-40] Virtually all monoclonal Ab on the market or in clinical development are IgG isotypes.[41] The finding that even modest concentrations of IgG may in theory effectively reinforce the mucosal barrier to minimize bacterial penetration strongly motivate further efforts to develop and evaluate passive immunization or therapy at mucosal surfaces with topically delivered IgG. Topical delivery to the mucosa, by concentrating the Ab directly at the sites of action, may actually reduce the total amount of Ab needed compared to systemic passive immunization. Furthermore, technological advances have already greatly reduced the cost of IgG production, and will likely lead to further cost reductions in the future. The

convergence of these factors will likely make IgG-based topical passive immunoprophylaxis or therapy at mucosal surfaces (such as the gut or female reproductive tract) cost-effective in the not too distant future.

Conclusion

Here, through rigorous computational modeling of complex kinetics and transport processes, we investigated the relative importance of agglutination vs. crosslinking individual bacteria to mucins in blocking bacterial permeation through mucus. Surprisingly, we found that IgG-mediated muco-trapping is nearly as effective as IgA-mediated agglutination in preventing bacterial penetration across physiologically-thick mucus layers. Given the stability and ease of manufacturing for IgG vs. sIgA, our work suggests that topical passive immunization of the GI mucosa is a practical alternative for reinforcing the mucus barrier against foreign pathogens.

Experimental Section

All parameters utilized in our model are listed in Table 1 and take the value listed unless otherwise noted.

Symbol	Value	Description	Reference
T	$1\ hr$	Simulation time	n/a
Δt	$0.0001s$	Time step	n/a
V	$40\ \mu m \times 40\ \mu m \times L_{mucus}\ \mu m$	Simulation volume	n/a
L_{mucus}	$50 - 450\ \mu m$	Thickness of mucus layer	[23]
N	80	Number of bacteria in V	n/a
L_{ba}	$3\ \mu m$	Length of bacterium	[42]
r_{ba}	$0.5\ \mu m$	Radius of bacterium as a capsule	[42]
S_{ba}	$9.4\ \mu m^2$	Surface area of a bacterium	Calculated from L_{ba} and r_{ba}
N_*	2000	Number of epitopes per bacteria	See text
v_0	$21 \mu m/s$	Native velocity of bacteria	Experimentally determined
μ_{run}	$0.9\ s$	Mean value of run duration	Experimentally determined
μ_{tumble}	$3.6\ s$	Mean value of tumble duration	Experimentally determined
α	0.8	Fraction of IgG freely diffusing at any instant in time	[13, 20-21]
β	0.99	Extent each Ab-mucin bond slows the velocity of bacteria	See text
L_{IgA}	$0.02\ \mu m$	Length of IgA	[43]
w_{IgA}	$390\ kDa$	Molecular weight of secretory IgA	[44]
k_{on}, k_{on}^f	$10^4\ M^{-1}s^{-1}$	Bacteria binding rate for Ab not associated with mucins	[45]
k_{on}^b	$k_{on}/100$	Bacteria binding rate for Ab associated with mucins	[44]
k_{off}	$5 \times 10^{-4} s^{-1}$	Ab unbinding rate from bacteria	[45]
C_{Ab}	$0.01 \sim 20\ \mu g/mL$	Ab concentration	[46]
D_{Ab}	$23\ \mu m/cm^2$	Diffusivity of Ab	[22]

Table 1. Model parameters.

Modeling the run and tumble motion of bacteria

We modeled each bacterium as a capsule composed of two semi-spherical caps of radius r on a cylinder of length a and radius r. A typical bacterium that is ~ 1 μm wide and ~ 3 μm long[42] would yield r = 0.5 μm, a = 2 μm, and a surface area ~9.4 μm^2. Naturally, the number of epitopes N_* that Ab can bind to on an individual bacterium varies substantially depending on both the antigen and bacterial species of interest. We conservatively assumed N_* to be 2000, or one epitope per ~4700 nm^2 on our model

bacterial surface. For comparison, there are roughly 200-400 copies of gD glycoprotein on an individual Herpes Simplex Virus[47-48], which translates to 1 epitope per ~630 nm^2, or roughly 7.5-fold greater density. Our base case includes simulation of 80 bacteria in a 40 μm x 40 μm x 50 μm domain of a mucus layer, corresponding to a bacterial concentration of 10^9/mL.

Bacteria frequently propel themselves using their flagella while alternating between run and tumble phases.[49-51] During a run phase, the flagella on a bacterium propel the bacterium in a set direction with a defined velocity; during the tumble phase, the bacterium stops swimming and rotates through a random angle. An approach commonly used to model bacterial chemotaxis is to calculate the tumbling probability at each iteration and use the rejection method to determine whether one bacterium runs or tumbles at that time step.[49-53] This allows simulating chemotactic bacterium to more frequently run along a nutrient gradient and more frequently tumble along a toxin gradient. Since our work does not involve chemotaxis and we assume the fluid environment to be isotropic, we simulated both run and tumble phases as exponential distributions with mean $\mu_{run} = 1/\lambda_{run} = 0.9\ s$ and $\mu_{tumble} = 1/\lambda_{tumble} = 3.6\ s$, values that were derived from tracking the motion of *Salmonella typhimurium* bacteria in mouse GI mucus. The run duration t has the probability density $f(t) = \lambda_{run} e^{-\lambda_{run} t}$ for $t \geq 0$. We assume all bacteria are in the run phase initially (Supplemental Figure 3). The duration of one run is determined as follows: select a random number s in $U(0,1)$, i.e., uniformly distributed in interval $(0,1)$, and the duration of this run phase is then set to be $-\log(s)/\lambda_{run}$. In a similar manner we can obtain a sample time interval for the tumble duration. The run and tumble phases can therefore be simulated alternately.

Initially, each bacterium is uniformly distributed in the upper $5\ \mu m$ of the mucus layer (relative to the epithelium), with random orientations. During the run phase, each bacterium swims along the direction of its current orientation under its current velocity. Initially no Ab are bound to any bacteria so the swimming velocity is $v_0 = 21\ \mu m/s$. During the tumble phase, the bacterium rotates about its center with a uniformly distributed angle sampled in three-dimensional space. We impose a 3D simulation domain V. Periodic boundary conditions are imposed in the x,y coordinates transverse to the layer thickness coordinate z, consisting of a 40 μm x 40 μm cross-section extended periodically. We designated the bottom of the mucus layer $z = 0\ \mu m$ to obtain a lower bound. We designated the top of the mucus layer $z = L_{mucus}$.

Ab binding and unbinding on bacteria

As described previously,[13, 20-21, 54] Ab can interact with mucins. The affinity of their interactions was previously approximated as $\alpha = m_{off}/(m_{off} + C_{Ab} m_{on})$, which reflects the fraction of Ab

associated versus unassociated with mucins, with m_{on} and m_{off} denoting the kinetic rates of Ab binding to and unbinding from mucins, respectively, with $\mathrm{C_{Ab}}$ denoting the Ab concentration.[22, 55] Since the molar quantities of Ab are far in excess of bacteria, we assume the Ab concentration C_{Ab} to be constant throughout the simulation; i.e., Ab depletion is negligible. We assume further that each bacterium-bound Ab associates with mucins independently, so that the aggregate effect of Ab-mucin affinity on effective bacterial motility is to multiply the bacterial swimming velocity by β^n, where n is the number of Ab bound to the individual bacterium, and β represents the extent to which a single Ab-mucin bond can slow bacterial velocity. Therefore, as *n* Ab accumulate on a bacterium, the swimming velocity is reduced to $v = \beta^n v_0$. The active motility of self-propelling bacteria vs. Brownian motion of viruses implies $\beta > \alpha$, where α reflects the fraction of time an Ab is dissociated from mucins ($\alpha = 1$ when no Ab associate with mucins, $\alpha = 0$ when all Ab associate with mucins). IgG and IgA in human mucus are previously measured to be associated with mucins ~10-20% of the time, i.e., $\alpha = 0.8 - 0.9$. Unfortunately, the extent to which a single bacterium-bound IgG may slow bacterial motility when transiently associated to mucin is not known. To make a conservative first-order approximation, we assume $\beta = 0.99$ in our model.

The binding and unbinding kinetics of Ab to an individual bacterium are modeled as described previously.[44, 56] The probability for an additional Ab to accumulate on a bacterium is dependent on the surrounding Ab concentration, the number of unoccupied binding sites on the bacterium, and the binding kinetic rate k_{on}. The probability for an Ab to unbind from a bacterium is dependent on the number of bound Ab and the unbinding rate k_{off}. When an Ab is bound to mucin, the diffusivity for the mucin-bound Ab is negligible compared with a free Ab. To account for the resulting decrease in collision frequency and consequently slower binding rate between mucin-bound Ab and bacteria, we approximate the binding rate for mucin-bound Ab as $k_{on}^b = k_{on}/100$. For a bacterium with n Ab bound, the probability for an additional Ab binding in a small time interval Δt is thus $P_{attach} = (N_* - n)\left(k_{on}^f u_f + k_{on}^b u_b\right)\Delta t$, and the probability for unbinding one Ab is $P_{detach} = n k_{off}\Delta t$, where u_f, u_b are mucin-free and mucin-bound Ab concentrations, respectively. In each iteration, we use a rejection method to determine whether a bacterium gains or loses one Ab or maintains the same number of Ab, i.e., sample s from $U(0,1)$, if $s < P_{attach}$, the bacterium gains one Ab, else if $s < P_{attach} + P_{detach}$, the bacterium loses one Ab, otherwise the number of Ab on the bacterium remains the same.

Agglutination Probability

For successful agglutination between two bacteria ba_1, ba_2, the distance between these two bacteria must be close enough (less than the length of a crosslinking Ab such as sIgA) and an Ab on one

bacterium must associate with an unoccupied antigenic epitope on the proximal bacterium. Therefore, we can roughly estimate this probability in terms of the number of Ab bound to each bacterium, i.e.,

$$P_{Agglu}(ba_1, ba_2) \propto n_1(N_* - n_2) + n_2(N_* - n_1)\,, \qquad (1)$$

where ba_1, ba_2 are within a distance of L_{IgA}, n_1, n_2 are the number of Ab bound to ba_1, ba_2, respectively. This is derived from the intuition that each Ab already bound to ba_1 shares the same probability to bind to ba_2, and each unoccupied binding site on ba_2 shares the same probability to bind an Ab on ba_1. Note that in an isotropic Ab concentration environment, n_1, n_2 are approximately equal; assuming $n_1 = n_2$, the optimal probability P_{opt} occurs at $n_1 = n_2 = N_*/2$. Therefore, for simplicity we fix P_{opt} and adjust P_{Agglu} proportionally according to equation (1).

Mice

Animals were purchased from Jackson Laboratory (C57B/6J, Stock No. 000664; B6.129S7-Rag1, Stock No. 002216). Mice were bred and maintained at the University of North Carolina Chapel Hill animal facility. All mice were age- and sex-matched and used between 8-10 weeks of age. All experiments were approved by the University of North Carolina Institutional Animal Care and Use Committee (IACUC ID 15-327).

GIM Collection

Mice were fasted for four hours to reduce the amount of luminal solid content in the gastrointestinal tract before being sacrificed for mucus collection. The small intestine was excised and slit open lengthwise. To collect GIM, the smooth surface of a glass capillary pipette (Wiretrol®, Drummond Scientific) was used to gently scrape along gastrointestinal tissue surface. Any remaining fecal solids were separated and mouse gastrointestinal mucus (mGIM) was kept in a microcentrifuge tube on ice or at 4°C until use within 24 hours.[57]

Bacterial Strain and Growth Condition.

The bacterial strain used in this study was a green fluorescent protein (GFP)-expressing *Salmonella typhimurium* SL1344 (provided by Dr. Ed Miao at the University of North Carolina Chapel Hill). SL1344-GFP was grown overnight at a shaking rate of 200 rpm at 37 °C in Luria-Bertani (LB) broth

supplemented with 50 µg/mL kanamycin for 14-16 hrs. Prior to microscopy, bacteria were diluted 1:10 and sub-cultured for an additional 2.5 hrs to ensure bacterial motility. Optical density (OD) 600 was measured using a NanoDrop One instrument from ThermoScientific. Bacterial motility in buffer was verified using a fluorescence microscope prior to study in mucus.

Sample Preparation for Particle Tracking Studies

Mucus slides for particle tracking were prepared using a custom-made, 10 µL slide chamber. Whole mucus was measured using a 20 µL glass capillary pipette. Five microliters of mGIM were transferred to the center of the slide chamber. Then,2.5 µL of either mouse IgG1 anti-LPS (Virostat 6331) or mouse IgG1 anti-biotin (Vector Labs, MB-9100) were pipetted directly onto the surface of the mucus and mixed into the sample by gently stirring with a pipette tip to ensure uniform distribution. Next, 2.5 µL of motile *Salmonella* culture was added to the mixture and again gently stirred. The final antibody concentration in mucus was 5 µg/mL. A coverslip was used to seal the well without significant compression of the mucus surface and quickly sealed with superglue to minimize sample dehydration. Prepared slides were incubated at 37°C for 15-30 minutes prior to imaging.

Fluorescence Particle Tracking Microscopy

We used high resolution multiple particle tracking to record and quantify the motion of hundreds of individual fluorescent *Salmonella typhimurium* in mGIM. Specifically, the translational motions of the bacteria were recorded using an EMCCD camera (Evolve 512; Photometrics, Tucson, AZ) mounted on an inverted epifluorescence microscope (AxioObserver D1; Zeiss, Thornwood, NY), equipped with an Alpha Plan Apo 100x/1.46 NA objective, environmental (temperature and CO_2) control chamber and an LED light source (Lumencor Light Engine DAPI/GFP/543/623/690). Videos (512 × 512, 16-bit image depth) were captured with MetaMorph imaging software (Molecular Devices, Sunnyvale, CA) at a temporal resolution of 57 ms and spatial resolution of 10 nm (nominal pixel resolution 0.156 µm/pixel) for 10 s. At least five independent videos were captured per sample to ensure that bacteria

were well-distributed over the entire surface. Trajectories of at least fifty individual bacteria were analyzed for each condition.[58] All experiments were performed at 37°C.

Analysis of Salmonella Motion

Image stacks acquired as described above were analyzed to extract the x and y positions of each *Salmonella* over time using a recently developed convolutional neural network.[59] Image stacks where directional drift of all particles was observed were excluded from analysis. This was determined visually by watching the time-lapse images and noting when all particles in the field moved in the same direction. To classify each increment of each track as either swimming, tumbling, or immobilized, we employed the widely used Hidden Markov Model framework, with the Expectation-Maximization algorithm for all inferences.[12, 22, 55] The Hidden-Markov Model framework has been used in particle tracking analysis for a range of applications.[60-62] We used a three-state Markov process to model the state-dependent motion of bacteria. Models of this type are referred to as stochastic hybrid models in the modeling literature and Gaussian mixture models in the statistics literature. The three motion states are swimming, in which motion is directed with a random direction; tumbling, in which motion is undirected and diffusive; and immobilized, in which motion is also undirected but substantially hindered (Supplemental Figure 4). We did not constrain the model to assign a smaller diffusion coefficient to the stuck state; nevertheless, the Maximum Likelihood stage of the Expectation-Maximization algorithm selected a diffusivity that was ~10 times less than the tumbling state (Table 2). Motion in the swimming state was modeled as directed with a single speed magnitude and a three-dimensional random direction. The random direction was selected uniformly over the unit sphere upon each transition from the tumble state into the swimming state. In total, the model contained eight parameters: the swim speed, the three state-specific diffusion coefficients, and four transition rates controlling the stochastic dynamics of switching between the three motion states. Transitions were allowed bidirectionally between the stuck and tumble states and between the tumble and swim states.

Antibody Treatment	$k_{stuck-tumble}$	$k_{tumble-stuck}$	$k_{tumble-swim}$	$k_{swim-tumble}$	Swim Speed	D_{stuck}	D_{tumble}	D_{swim}
No Exogenous Ab	0.57	0.49	0.37	1.2	18.7	0.03	0.18	1.1
IgG anti-biotin	0.61	0.47	0.37	1.3	18.1	0.03	0.18	1.1
IgG anti-LPS	0.56	0.50	0.25	2.4	15.3	0.02	0.18	1.1
IgG anti-LPS deglycosylated	0.57	0.48	0.39	1.3	18.6	0.03	0.18	1.1

Table 2: Maximum likelihood parameter estimates

Ancillary Information

Supporting Information

Supplemental Figures: Effect of IgG on bacteria penetration across mucus; Distribution of distances for bacteria to its closest neighbor at various time points
Supplemental Video 1: *Salmonella typhimurium* in mouse GI
Supplemental Video 2: *Salmonella typhimurium* in mouse GI treated with anti-LPS IgG

Corresponding authors

Samuel K. Lai	T. (919) 966-3024	E. lai@unc.edu
M. Gregory Forest	T. (919) 962-9606	E. forest@unc.edu

Current Author Addresses

Feifei Xu: Google, Inc., Irvine, CA 92612
Jay M. Newby: University of Alberta, Edmonton, AB, Canada T6G 2R3
Holly A. Schroeder: Asklepios Biopharmaceuticals, RTP, NC 27709
Timothy Wessler: University of Michigan, Ann Arbor, MI 48109
Alex Chen: General Electric Global Research Center, Niskayuna, NY 12309

Author Contributions

FX, JMN, MGF, and SKL conceptualized and designed the presented idea. HAS executed the experiments. FX, JMN, TW, and AC performed the simulations. FX, JMN, JLS, HAS, MGF, and SKL analyzed the data and wrote and edited the paper.

Acknowledgements

This work was supported by the National Institutes of Health (https://www.nih.gov/) grant R56HD095629 (SKL); the National Science Foundation (https://www.nsf.gov/) grants DMR-1810168 (SKL), DMS-1462992 (MGF, JMN, FX), DMS-1664645 (MGF), and DMS-1816630 (MGF, JMN); The David and Lucile Packard Foundation (https://www.packard.org/) 2013-39274 (SKL); The Eshelman Institute for Innovation (https://unceii.org/, SKL); and startup funds from the University of North Carolina Eshelman School of Pharmacy (https://pharmacy.unc.edu/; SKL). The funders had no role in study design, data collection and analysis, decision to publish, or manuscript preparation.

Conflict of Interest Statement

Intellectual property associated with harnessing antibody-mucin interactions described in part in this publication was developed at the University of North Carolina - Chapel Hill (UNC-CH) and has been licensed to Inhalon Biopharma, Inc and Mucommune, LLC. SKL is a founder of both Inhalon and Mucommune and currently serves as the interim CEO and on the board of directors and scientific advisory board at both companies. SKL owns company stock; SKL's relationship with Inhalon and Mucommune is subject to certain restrictions under University policy. The terms of this arrangement are being managed by UNC-CH in accordance with its conflict of interest policies.
The technology behind the neutral-network based tracking analysis described in part in this publication was developed at University of North Carolina - Chapel Hill (UNC-CH) and has been licensed to AI Tracking Solutions, LLC. JMN, MGF, and SKL are co-founders of AITS solutions and serve on the board of

directors. JMN, MGF, and SKL all own company stock; MGF's and SKL's relationships with AI Tracking Solutions are subject to certain restrictions under University policy. The terms of this arrangement are being managed by UNC-CH in accordance with its conflict of interest policies.

Abbreviations

Ab	antibodies
GFP	green fluorescent protein
GI	gastrointestinal ,
LB	Luria Broth
mGIM	mouse GI mucus
OD600	optical density at 600 nm
sIgA	secretory IgA

References

1. Lai, S. K.; Wang, Y.-Y.; Wirtz, D. and Hanes, J. (2009) Micro- and macrorheology of mucus. *Adv. Drug Del. Rev.* 61 (2), 86-100. 10.1016/j.addr.2008.09.012.
2. Mathias, A.; Pais, B.; Favre, L.; Benyacoub, J. and Corthésy, B. (2014) Role of secretory IgA in the mucosal sensing of commensal bacteria. *Gut Microbes.* 5 (6), 688-695. 10.4161/19490976.2014.983763.
3. Rogier, E. W.; Frantz, A. L.; Bruno, M. E. and Kaetzel, C. S. (2014) Secretory IgA is concentrated in the outer layer of colonic mucus along with gut bacteria. *Pathogens.* 3 (2), 390-403. 10.3390/pathogens3020390.
4. Daniele, R. P. (1990) Immunoglobulin secretion in the airways. *Annu. Rev. Physiol.* 52, 117-195. 10.1146/annurev.ph.52.030190.001141.
5. Usala, S. J.; O'Brien Usala, F.; Haciski, R.; Holt, J. A. and Schumacher, G. F. B. (1989) IgG and IgA content of vaginal fluid during the menstrual cycle. *J. Reprod. Med.* 34 (4), 292-294.
6. Macpherson, A. J. and McCoy, K. D. (2013) Stratification and compartmentalisation of immunoglobulin responses to commensal intestinal microbes. *Semin. Immunol.* 25 (5), 358-363. 10.1016/j.smim.2013.09.004.
7. Agarwal, S. and Cunningham-Rundles, C. (2007) Assessment and clinical interpretation of reduced IgG values. *Ann. Allergy, Asthma Immunol.* 99 (3), 281-283. 10.1016/s1081-1206(10)60665-5.
8. Mestecky, J.; Russell, M. W. and Elson, C. O. (1999) Intestinal IgA: Novel views on its function in the defence of the largest mucosal surface. *Gut.* 44 (1), 2-5.
9. McSweegan, E.; Burr, D. H. and Walker, R. I. (1987) Intestinal mucus gel and secretory antibody are barriers to *Campylobacter jejuni* adherence to INT 407 cells. *Infect. Immun.* 55 (6), 1431-1435.
10. Biesbrock, A. R.; Reddy, M. S. and Levine, M. J. (1991) Interaction of a salivary mucin-secretory immunoglobulin A complex with mucosal pathogens. *Infect. Immun.* 59 (10), 3492-3497.
11. Magnusson, K.-E. and Sthernström, I. (1982) Mucosal barrier mechanisms. Interplay between secretory IgA (SIgA), IgG and mucins on the surface properties and association of salmonellae with intestine and granulocytes. *Immunology.* 45, 239-248.

12. McKinley, S. A.; Chen, A.; Shi, F.; Wang, S.; Mucha, P. J.; Forest, M. G. and Lai, S. K. (2014) Modeling neutralization kinetics of HIV by broadly neutralizing monoclonal antibodies in genital secretions coating the cervicovaginal mucosa. *PLoS One.* 9 (6), e100598. 10.1371/journal.pone.0100598.
13. Wang, Y.-Y.; Kannan, A.; Nunn, K. L.; Murphy, M. A.; Subramani, D. B.; Moench, T. R.; Cone, R. A. and Lai, S. K. (2014) IgG in cervicovaginal mucus traps HSV and prevents vaginal herpes infections. *Mucosal Immunol.* 7 (5), 1036-1044. 10.1038/mi.2013.120.
14. Wang, Y.-Y.; Harit, D.; Subramani, D. B.; Arora, H.; Kumar, P. A. and Lai, S. K. (2017) Influenza-binding antibodies immobilise influenza viruses in fresh human airway mucus. *Eur. Respir. J.* 49 (1), 1601709. 10.1183/13993003.01709-2016.
15. Yang, B.; Schaefer, A.; Wang, Y.-Y.; McCallen, J. D.; Lee, P.; Newby, J. M.; Arora, H.; Kumar, P. A.; Zeitlin, L.; Whaley, K. J.; McKinley, S. A.; Fischer, W. A., 2nd; Harit, D. and Lai, S. K. (2018) ZMapp reinforces the airway mucosal barrier against Ebola virus. *J. Infect. Dis.* 218 (6), 901-910. 10.1093/infdis/jiy230.
16. Sicard, J.-F.; Le Bihan, G.; Vogeleer, P.; Jacques, M. and Harel, J. (2017) Interactions of intestinal bacteria with components of the intestinal mucus. *Front. Cell. Infect. Microbiol.* 7, 387. 10.3389/fcimb.2017.00387.
17. Rossez, Y.; Wolfson, E. B.; Holmes, A.; Gally, D. L. and Holden, N. J. (2015) Bacterial flagella: Twist and stick, or dodge across the kingdoms. *PLoS Pathogens.* 11 (1), e1004483. 10.1371/journal.ppat.1004483.
18. Stecher, B.; Barthel, M.; Schlumberger, M. C.; Haberli, L.; Rabsch, W.; Kremer, M. and Hardt, W.-D. (2008) Motility allows *S. Typhimurium* to benefit from the mucosal defence. *Cell. Microbiol.* 10 (5), 1166-1180. 10.1111/j.1462-5822.2008.01118.x.
19. Dempster, A. P.; Laird, N. M. and Rubin, D. B. (1977) Maximum likelihood from incomplete data via the EM algorithm. *J. Roy. Stat. Soc. Ser. B. (Stat. Method.).* 39 (1), 1-38.
20. Saltzman, W. M.; Radomsky, M. L.; Whaley, K. J. and Cone, R. A. (1994) Antibody diffusion in human cervical mucus. *Biophys. J.* 66, 506-515. 10.1016/S0006-3495(94)80802-1.
21. Olmsted, S. S.; Padgett, J. L.; Yudin, A. I.; Whaley, K. J.; Moench, T. R. and Cone, R. A. (2001) Diffusion of macromolecules and virus-like particles in human cervical mucus. *Biophys. J.* 81, 1930-1937. 10.1016/S0006-3495(01)75844-4.
22. Wessler, T.; Chen, A.; McKinley, S. A.; Cone, R.; Forest, M. G. and Lai, S. K. (2016) Using computational modeling to optimize the design of antibodies that trap viruses in mucus. *ACS Infect. Dis.* 2 (1), 82-92. 10.1021/acsinfecdis.5b00108.
23. Atuma, C.; Strugala, V.; Allen, A. and Holm, L. (2001) The adherent gastrointestinal mucus gel layer: Thickness and physical state in vivo. *Am. J. Physiol. Gastrointest. Liver Physiol.* 280, G922:G929. 10.1152/ajpgi.2001.280.5.G922.
24. Michetti, P.; Mahan, M. J.; Slauch, J. M.; Mekalanos, J. J. and Neutra, M. R. (1992) Monoclonal secretory immunoglobulin A protects mice againt oral challenge with the invasve pathogen *Salmonela typhimurium*. *Infect. Immun.* 60 (5), 1786-1792.
25. Mantis, N. J.; Rol, N. and Corthésy, B. (2011) Secretory IgA's complex roles in immunity and mucosal homeostasis in the gut. *Mucosal Immunol.* 4 (6), 603-611. 10.1038/mi.2011.41.
26. Chen, A.; McKinley, S. A.; Shi, F.; Wang, S.; Mucha, P. J.; Harit, D.; Forest, M. G. and Lai, S. K. (2015) Modeling of virion collisions in cervicovaginal mucus reveals limits on agglutination as the protective mechanism of secretory immunoglobulin A. *PLoS One.* 10 (7), e0131351. 10.1371/journal.pone.0131351.

27. Bergstrom, K. S.; Kissoon-Singh, V.; Gibson, D. L.; Ma, C.; Montero, M.; Sham, H. P.; Ryz, N.; Huang, T.; Velcich, A.; Finlay, B. B.; Chadee, K. and Vallance, B. A. (2010) Muc2 protects against lethal infectious colitis by disassociating pathogenic and commensal bacteria from the colonic mucosa. *PLoS Pathogens.* 6 (5), e1000902. 10.1371/journal.ppat.1000902.
28. Zarepour, M.; Bhullar, K.; Montero, M.; Ma, C.; Huang, T.; Velcich, A.; Xia, L. and Vallance, B. A. (2013) The mucin Muc2 limits pathogen burdens and epithelial barrier dysfunction during *Salmonella enterica* serovar Typhimurium colitis. *Infect. Immun.* 81 (10), 3672-3693. 10.1128 /IAI.00854-13.
29. Hansson, G. C. (2012) Role of mucus layers in gut infection and inflammation. *Curr. Opin. Microbiol.* 15 (1), 57-62. 10.1016/j.mib.2011.11.002.
30. Lai, S. K.; Hida, K.; Shukair, S.; Wang, Y.-Y.; Figueiredo, A.; Cone, R.; Hope, T. J. and Hanes, J. (2009) Human immunodeficiency virus type 1 is trapped by acidic but not by neutralized human cervicovaginal mucus. *J. Virol.* 83 (21), 11196-11200. 10.1128/JVI.01899-08.
31. Nunn, K. L.; Wang, Y.-Y.; Harit, D.; Humphrys, M. S.; Ma, B.; Cone, R.; Ravel, J. and Lai, S. K. (2015) Enhanced trapping of HIV-1 by human cervicovaginal mucus Is associated with *Lactobacillus crispatus*-dominant microbiota. *MBio.* 6 (5), e01084-01015. 10.1128/mBio.01084-15.
32. Schroeder, H. A.; Nunn, K. L.; Schaefer, A.; Henry, C. E.; Lam, F.; Pauly, M. H.; Whaley, K. J.; Zeitlin, L.; Humphrys, M. S.; Ravel, J. and Lai, S. K. (2018) Herpes simplex virus-binding IgG traps HSV in human cervicovaginal mucus across the menstrual cycle and diverse vaginal microbial composition. *Mucosal Immunol.* 11, 1477-1486. 10.1038/s41385-018-0054-z.
33. Tamar, E.; Koler, M. and Vaknin, A. (2016) The role of motility and chemotaxis in the bacterial colonization of protected surfaces. *Sci. Rep.* 6, 19616. 10.1038/srep19616.
34. Bansil, R.; Celli, J. P.; Hardcastle, J. M. and Turner, B. S. (2013) The influence of mucus microstructure and rheology in *Helicobacter pylori* infection. *Front. Immunol.* 4, 310. 10.3389/fimmu.2013.00310.
35. Maurer, M. A.; Meyer, L.; Bianchi, M.; Turner, H. L.; Le, N. P. L.; Steck, M.; Wyrzucki, A.; Orlowski, V.; Ward, A. B.; Crispin, M. and Hangartner, L. (2018) Glycosylation of human IgA directly inhibits influenza A and other sialic-acid-binding viruses. *Cell Reports.* 23 (1), 90-99. 10.1016/j.celrep.2018.03.027.
36. Donaldson, G. P.; Ladinsky, M. S.; Yu, K. B.; Sanders, J. G.; Youu, B. B.; Chou, W.-C.; Conner, M. E.; Earl, A. M.; Knight, R.; Bjorkman, P. J. and Mazmanian, S. K. (2018) Gut microbiota utilize immunoglobulin A for mucosal colonization. *Science.* 360, 795-800. 10.1126/science.aaq0926.
37. Moor, K.; Diard, M. d. r.; Sellin, M. E.; Felmy, B.; Wotzka, S. Y.; Toska, A.; Bakkeren, E.; Arnoldini, M.; Bansept, F.; Dal Co, A.; Völler, T.; Minola, A.; Fernandez-Rodriguez, B.; Agatic, G.; Barbieri, S.; Piccoli, L.; Casiraghi, C.; Corti, D.; Lanzavecchia, A.; Regoes, R. R.; Loverdo, C.; Stocker, R.; Brumley, D. R.; Hardt, W.-D. and Slack, E. (2017) High-avidity IgA protects the intestine by enchaining growing bacteria. *Nature.* 544 (7651), 498-502. 10.1038/nature22058.
38. Hansen, I. S.; Baeten, D. L. P. and den Dunnen, J. (2019) The inflammatory function of human IgA. *Cell. Mol. Life Sci.* 76 (6), 1041-1055. 10.1007/s00018-018-2976-8.
39. Wycoff, K. L. (2005) Secretory IgA antibodies from plants. *Curr. Pharm. Des.* 11, 2429-2437. 10.2174/1381612054367508.
40. Cohen, G. and Eisenberg, H. (1969) Viscosity and sedimentation study of sonicated DNA-proflavine complexes. *Biopolymers.* 8, 45-55. 10.1002/bip.1969.360080105.

41. Marasco, W. A. and Sui, J. (2007) The growth and potential of human antiviral monoclonal antibody therapeutics. *Nat. Biotechnol.* 25 (12), 1421-1434. 10.1038/nbt1363.
42. Aldea, M.; Herrero, E. and Trueba, F. J. (1982) Constancy of diameter through the cell cycle of *Salmonella typhimurium* LT2. *Curr. Microbiol.* 7, 165-168. 10.1007/BF01568969.
43. Bonner, A.; Almogren, A.; Furtado, P. B.; Kerr, M. A. and Perkins, S. J. (2009) The nonplanar secretory IgA2 and near planar secretory IgA1 solution structures rationalize their different mucosal immune responses. *J. Biol. Chem.* 284 (8), 5077-5087. 10.1074/jbc.M807529200.
44. Egbert, M. D.; Barandiaran, X. E. and Di Paolo, E. A. (2010) A minimal model of metabolism-based chemotaxis. *PLoS Comp. Biol.* 6 (12), e1001004. 10.1371/.
45. Landry, J. P.; Ke, Y.; Yu, G. L. and Zhu, X. D. (2015) Measuring affinity constants of 1450 monoclonal antibodies to peptide targets with a microarray-based label-free assay platform. *J. Immunol. Methods.* 417, 86-96. 10.1016/j.jim.2014.12.011.
46. Ferguson, A., (1999) Overview of gut mucosal injury and immunopathology. In *Mucosal Immunol.*, 2 ed.;pp 993-1005. Ogra, P. L.; Metstecky, J.; Lamm, M. E.; Strober, W.; Bienenstock, J. and McGhee, J. R., Eds. Academic Press: New York, 1999;
47. Clarke, R. W.; Drews, A.; Browne, H. and Klenerman, D. (2013) A single gD glycoprotein can mediate infection by Herpes simplex virus. *J. Am. Chem. Soc.* 135 (30), 11175-11180. 10.1021/ja4038406.
48. Clarke, R. W.; Monnier, N.; Li, H.; Zhou, D.; Browne, H. and Klenerman, D. (2007) Two-color fluorescence analysis of individual virions determines the distribution of the copy number of proteins in herpes simplex virus particles. *Biophys. J.* 93 (4), 1329-1337. 10.1529/biophysj.107.106351.
49. Berg, H. C. and Turner, L. (1990) Chemotaxis of bacteria in glass capillary arrays. *Biophys. J.* 58, 919-930. 10.1016/S0006-3495(90)82436-X.
50. Brown, D. A. and Berg, H. C. (1974) Temporal stimulation of chemotaxis in *Escherichia coli*. *Proc. Natl. Acad. Sci. U. S. A.* 71 (4), 1399-1392. 10.1073/pnas.71.4.1388.
51. Berg, H. C. (1975) Bacterial behaviour. *Nature.* 254, 389-392.
52. Hammond, S. M.; Lambert, P. A. and Rycroft, A. N. *The Bacterial Cell Surface*. Springer Netherlands: 1984.
53. Macnab, R. A. and Koshland, D. E., Jr. (1972) The gradient-sensing mechanism in bacterial chemotaxis. *Proc. Natl. Acad. Sci. U. S. A.* 69 (9), 2509-2512.
54. Wang, Y.-Y.; Schroeder, H. A.; Nunn, K. L.; Woods, K.; Anderson, D. J.; Lai, S. K. and Cone, R. A. (2016) Diffusion of immunoglobulin G in shed vaginal epithelial cells and in cell-free regions of human cervicovaginal mucus. *PLoS One.* 11 (6), e0158338. 10.1371/journal.pone.0158338.
55. Chen, A.; McKinley, S. A.; Wang, S.; Shi, F.; Mucha, P. J.; Forest, M. G. and Lai, S. K. (2014) Transient antibody-mucin interactions produce a dynamic molecular shield against viral invasion. *Biophys. J.* 106 (9), 2028-2036. 10.1016/j.bpj.2014.02.038.
56. Xu, F.; Bierman, R.; Healy, F. and Nguyen, H. (2016) A multi-scale model of *Escherichia coli* chemotaxis from intracellular signaling pathway to motility and nutrient uptake in nutrient gradient and isotropic fluid environments. *Comput. Math. Appl.* 71 (11), 2466-2478. 10.1016/j.camwa.2015.12.019.
57. Ensign, L. M.; Henning, A.; Schneider, C. S.; Maisel, K.; Wang, Y.-Y.; Porosoff, M. D.; Cone, R. A. and Hanes, J. (2013) *Ex vivo* characterization of particle transport in mucus

secretions coating freshly excised mucosal tissues. *Mol. Pharm.* 10 (6), 2176-2182. 10.1021/mp400087y.
58. Wang, Y.-Y.; Lai, S. K.; Ensign, L. M.; Zhong, W.; Cone, R. A. and Hanes, J. (2013) The microstructure and bulk rheology of human cervicovaginal mucus are remarkably resistant to changes in pH. *Biomacromolecules.* 14 (12), 4429-4435. 10.1021/bm401356q.
59. Newby, J. M.; Schaefer, A. M.; Lee, P. T.; Forest, M. G. and Lai, S. K. (2018) Convolutional neural networks automate detection for tracking of submicron scale particles in 2D and 3D. *Proc. Natl. Acad. Sci. U. S. A.* 115 (36), 9026-9031. 10.1073/pnas.1804420115.
60. Das, R.; Cairo, C. W. and Coombs, D. (2009) A hidden Markov model for single particle tracks quantifies dynamic interactions between LFA-1 and the actin cytoskeleton. *PLoS Comp. Biol.* 5 (11), e1000556. 10.1371/journal.pcbi.1000556.
61. Abraham, L.; Lu, H. Y.; Falcão, R. C.; Scurll, J.; Jou, T.; Irwin, B.; Tafteh, R.; Gold, M. R. and Coombs, D. (2017) Limitations of Qdot labelling compared to directly-conjugated probes for single particle tracking of B cell receptor mobility. *Sci. Rep.* 7 (1), 11379. 10.1038/s41598-017-11563-9.
62. Johnson, S.; van de Meent, J.-W.; Phillips, R.; Wiggins, C. H. and Lindén, M. (2014) Multiple LacI-mediated loops revealed by Bayesian statistics and tethered particle motion. *Nucleic Acids Res.* 42 (16), 10265-10277. 10.1093/nar/gku563.